

Discovery of a geomorphological analog to Martian araneiforms in the Qaidam Basin, Tibetan Plateau

Shengxing Zhang^{1,2,3}, Yiliang Li^{2,3} ✉, and Wei Leng^{1,3} ✉

¹Laboratory of Seismology and Physics of Earth's Interior, School of Earth and Space Sciences, University of Science and Technology of China, Hefei 230026, China;

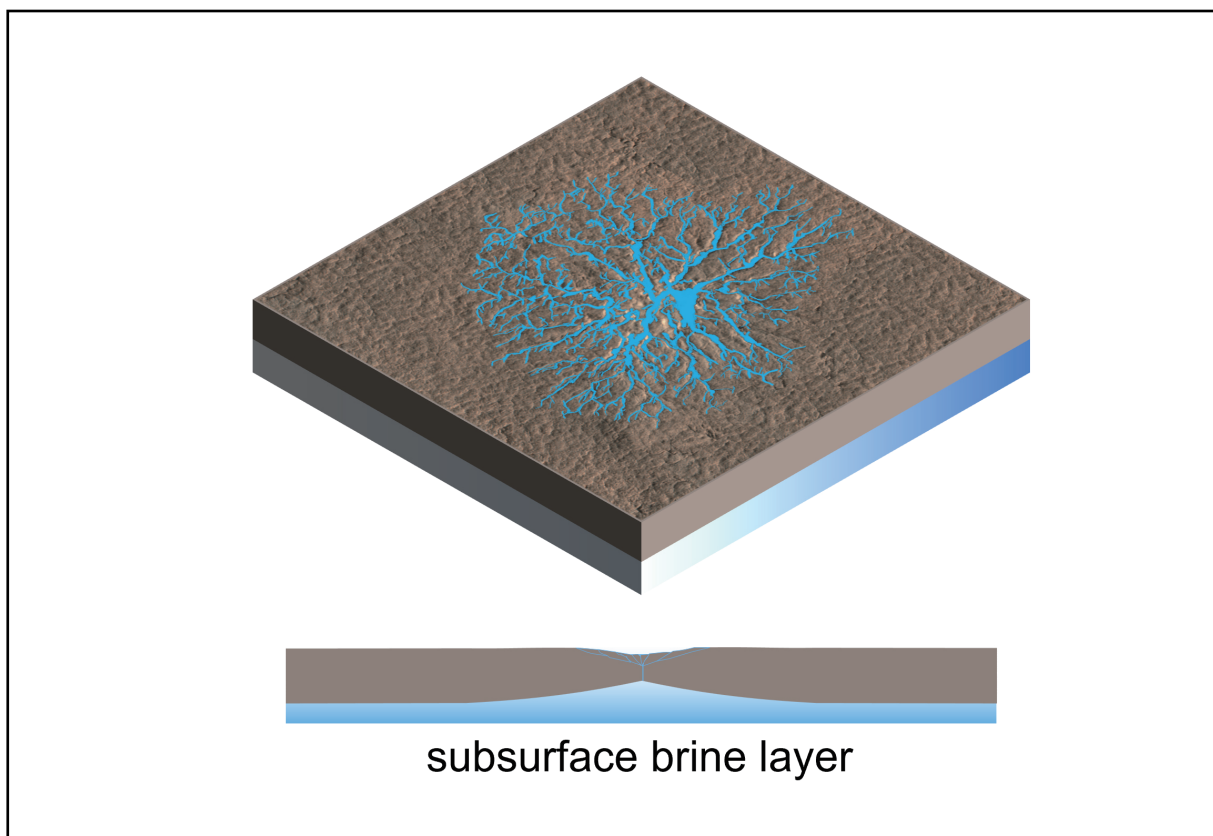
²Department of Earth Sciences, The University of Hong Kong, Hong Kong 999077, China;

³CAS Center for Excellence in Comparative Planetology, Hefei 230026, China

✉Correspondence: Yiliang Li, E-mail: yiliang@hku.hk; Wei Leng, E-mail: wleng@ustc.edu.cn

© 2024 The Author(s). This is an open access article under the CC BY-NC-ND 4.0 license (<http://creativecommons.org/licenses/by-nc-nd/4.0/>).

Graphical abstract



Araneiforms on Earth and Mars may have a similar saltwater-related origin.

Public summary

- The first terrestrial analog for martian araneiforms was identified in the Qaidam Basin, Tibetan Plateau.
- Quantitative geomorphological analysis has demonstrated the similar fractal features between Qaidam and martian araneiforms.
- The formation of araneiforms can be explained by the erosion of upwelling salt water from the subsurface.

Discovery of a geomorphological analog to Martian araneiforms in the Qaidam Basin, Tibetan Plateau

Shengxing Zhang^{1,2,3}, Yiliang Li^{2,3} ✉, and Wei Leng^{1,3} ✉

¹Laboratory of Seismology and Physics of Earth's Interior, School of Earth and Space Sciences, University of Science and Technology of China, Hefei 230026, China;

²Department of Earth Sciences, The University of Hong Kong, Hong Kong 999077, China;

³CAS Center for Excellence in Comparative Planetology, Hefei 230026, China

✉ Correspondence: Yiliang Li, E-mail: yiliang@hku.hk; Wei Leng, E-mail: w leng@ustc.edu.cn

© 2024 The Author(s). This is an open access article under the CC BY-NC-ND 4.0 license (<http://creativecommons.org/licenses/by-nc-nd/4.0/>).



Cite This: *JUSTC*, 2024, 54(5): 0501 (9pp)



Read Online



Supporting Information

Abstract: Araneiforms are spider-like ground patterns that are widespread in the southern polar regions of Mars. A gas erosion process driven by the seasonal sublimation of CO₂ ice was proposed as an explanation for their formation, which cannot occur on Earth due to the high climatic temperature. In this study, we propose an alternative mechanism that attributes the araneiform formation to the erosion of upwelling salt water from the subsurface, relying on the identification of the first terrestrial analog found in a playa of the Qaidam Basin on the northern Tibetan Plateau. Morphological analysis indicates that the structures in the Qaidam Basin have fractal features comparable to araneiforms on Mars. A numerical model is developed to investigate the araneiform formation driven by the water-diffusion mechanism. The simulation results indicate that the water-diffusion process, under varying ground conditions, may be responsible for the diverse araneiform morphologies observed on both Earth and Mars. Our numerical simulations also demonstrate that the orientations of the saltwater diffusion networks are controlled by pre-existing polygonal cracks, which is consistent with observations of araneiforms on Mars and Earth. Our study thus suggests that a saltwater-related origin of the araneiform is possible and has significant implications for water searches on Mars.

Keywords: araneiform landform; subsurface water; Qaidam Basin; Mars analog; fractal simulations

CLC number: P931

Document code: A

1 Introduction

Araneiforms (or colloquially spiders) are fractal landforms with branching channels^[1–5]. They were initially identified through orbital observations in the high southern latitudes of Mars^[6–10]. The High Resolution Imaging Science Experiment (HiRISE) has captured many high-quality images of Martian araneiforms in recent years (Fig. S1). A typical Martian spider is composed of radial dendritic troughs (Figs. 1a–d)^[2,11]. Their formation is thought to be a progressive erosion process^[3], that ranges from the early state (Fig. 1a) with a few branches to the mature state (Fig. 1c) with up to thousands of branches. Depending on the extent of erosion, the diameter scale of the structure varies from ~10 m in the early stage (Fig. 1a) to ~10² m in the middlestage (Fig. 1b) and up to ~10³ m in the mature stage (Fig. 1c). For some araneiforms, HiRISE can even detect their continuous growth with newly sprouting branches during the observation period^[3], implying that their formation mechanism is still functioning on present-day Mars.

A recent theory suggests that the formation of Martian araneiforms is triggered by seasonal sublimation jets of CO₂^[1, 4, 5, 12, 13]. This gas erosion model assumes the existence of a seasonally translucent CO₂ ice sheet overlying the unconsolidated regolith substrate^[5]. When the warm spring arrives,

sunlight can penetrate the ice sheet, heating the underlying substrate and causing basal sublimation of CO₂. Driven by the pressure difference, CO₂ trapped under the ice cap moves explosively to weak spots in the ice layer and spews out. The movement of the gas under the ice cuts the substrate and forms pits and troughs. The repetition of seasonal gas jetting at the same location leads to further growth of these erosion troughs and could explain the observed spider-like structures on Mars^[3, 11, 12]. According to this scenario, the occurrence of seasonal CO₂ ice sheets on the much warmer Earth is impossible, and therefore, it is claimed that there is no analogous process^[2, 11].

Although laboratory experiments with gas-jetting settings can produce the typical starburst structure (i.e., Figs. 1a–c), radial symmetry is not an inherent feature of araneiforms. There are many other araneiform morphologies^[1, 2], most of which have not been tested by gas-jetting experiments and for which there is no convincing explanation. For instance, some parallel araneiform troughs are observed overgrowing a ditch (Fig. 1e). Their direction of growth is perpendicular to the ditch, akin to tributaries branching off the mainstream^[14]. There are also some crisscrossing araneiforms (Fig. 1f) with meandering and wide channels like trickles. The direction of these channels could also be influenced by the local wind direction, as shown by the preserved shaded tails (Fig. 1f). At

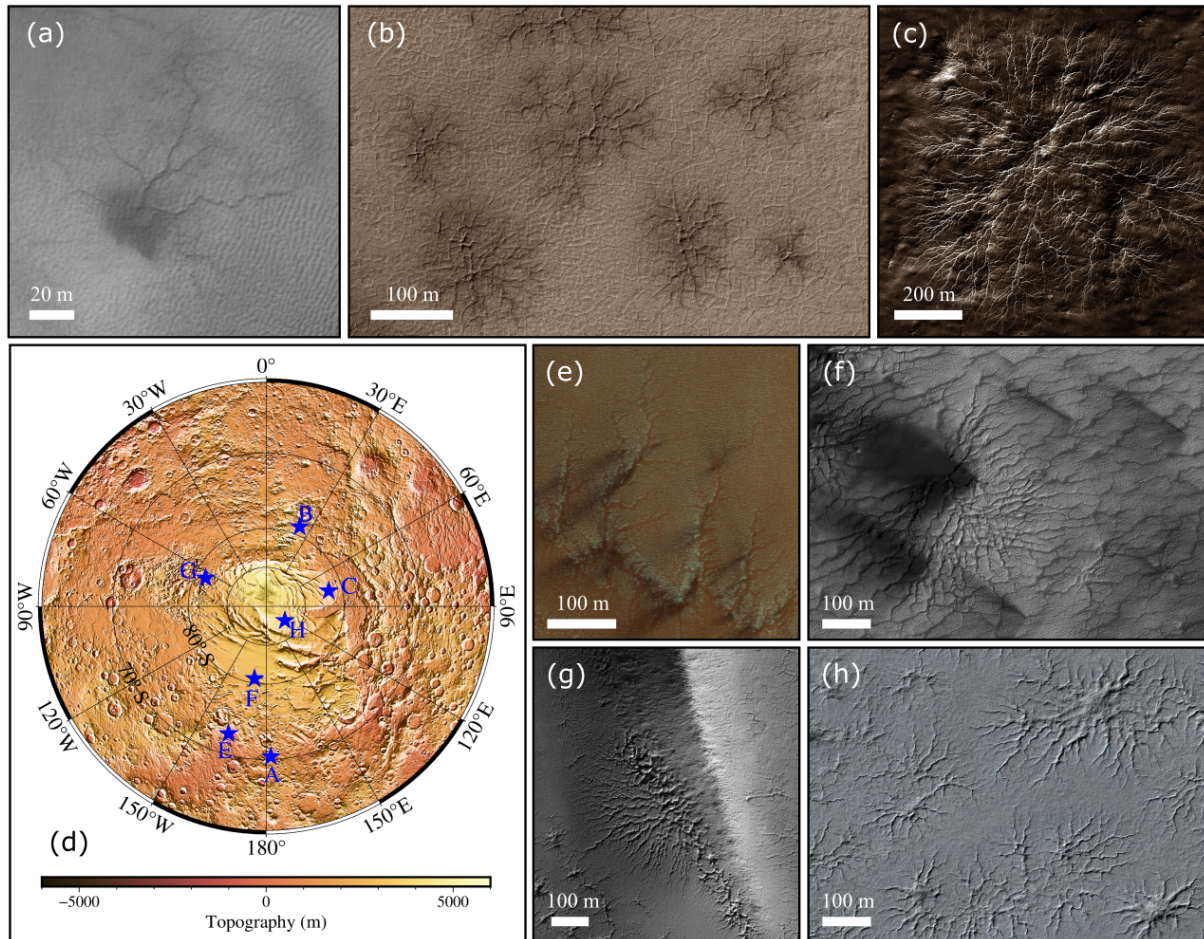


Fig. 1. Various araneiform morphologies were observed in the south polar region of Mars. (a) The early stage of the araneiform (ESP_023600_1095). (b) The middle stage of the araneiform (ESP_066587_0790). (c) The mature stage of the Martian araneiform with a good fractal structure (ESP_014255_0980). (d) The shaded relief map of the south polar region of Mars. The blue stars represent the locations of the corresponding araneiforms. (e) Parallel araneiforms that developed along a ditch (ESP_056038_1070). (f) Araneiform networks with meandering and wide channels (ESP_029613_0995). (g) The half araneiform developed under a dune (PSP_006204_0985). (h) Fat araneiforms (ESP_066555_0870).

the lower edge of a dune, some structures grow on one side (Fig. 1g), referred to as “half spiders”^[1]. Their growth on the dune side is seemingly impeded by the high topography. Additionally, some araneiforms have large pits in the center, previously termed “fat spiders” (Fig. 1h)^[1].

Another puzzle with the Martian araneiforms is their twisted morphologies, which form on polygonal terrains. Polygonal terrain refers to the ground covered with regular or irregular polygonal cracks and typically occurs on dried lands or playas^[15]. Numerous polygonal terrains have been identified in the southern hemisphere of Mars, many of which are accompanied by araneiforms (e.g., Fig. 2). Unlike the conventional staggered and radial patterns, the araneiform channels formed on these terrains strongly overlap with the polygonal fractures. With different polygonal geometries, the overlying araneiform networks also exhibit different patterns (Fig. 2).

In this study, we report the first araneiform analog on Earth and clarify that the mechanism of water erosion can be used to explain the origin of Martian araneiforms with diverse morphologies. Furthermore, we formulate a numerical model to simulate the growth of araneiforms on a pre-existing polygonal terrain and discuss the genesis of the characteristic araneiform morphology observed on Mars and Earth.

2 Materials and methods

2.1 Geologic settings of the Qaidam spider terrain

Through fieldwork conducted in the Qaidam Basin, we have identified the first terrestrial analog of the Martian araneiforms, which we have dubbed Qaidam spiders. The Qaidam Basin is situated in the northern Tibetan Plateau and is the highest intermountain basin on Earth; it is surrounded by the Qilian Mountains to the east, the Kunlun Mountains to the south, and the Altun Mountains to the north^[16,17] (Fig. 3a). The hyperarid climate of the basin, characterized by extremely low precipitation and high evaporation rates, has led to soil salinization and the widespread presence of salt lakes or subsurface salt solutions^[17,18]. Many of the geomorphological features that have formed under these environmental conditions are strikingly similar to those found on Mars^[17,19], making the Qaidam Basin a highly valuable analog site for studying Martian surface processes. The Qaidam spider terrain is located on the desiccated floor of Lake Taijinaier, an endorheic salt lake on the periphery of an alluvial fan^[20] (Fig. 3b). We observed various spider-like structures on the site (Fig. 4).

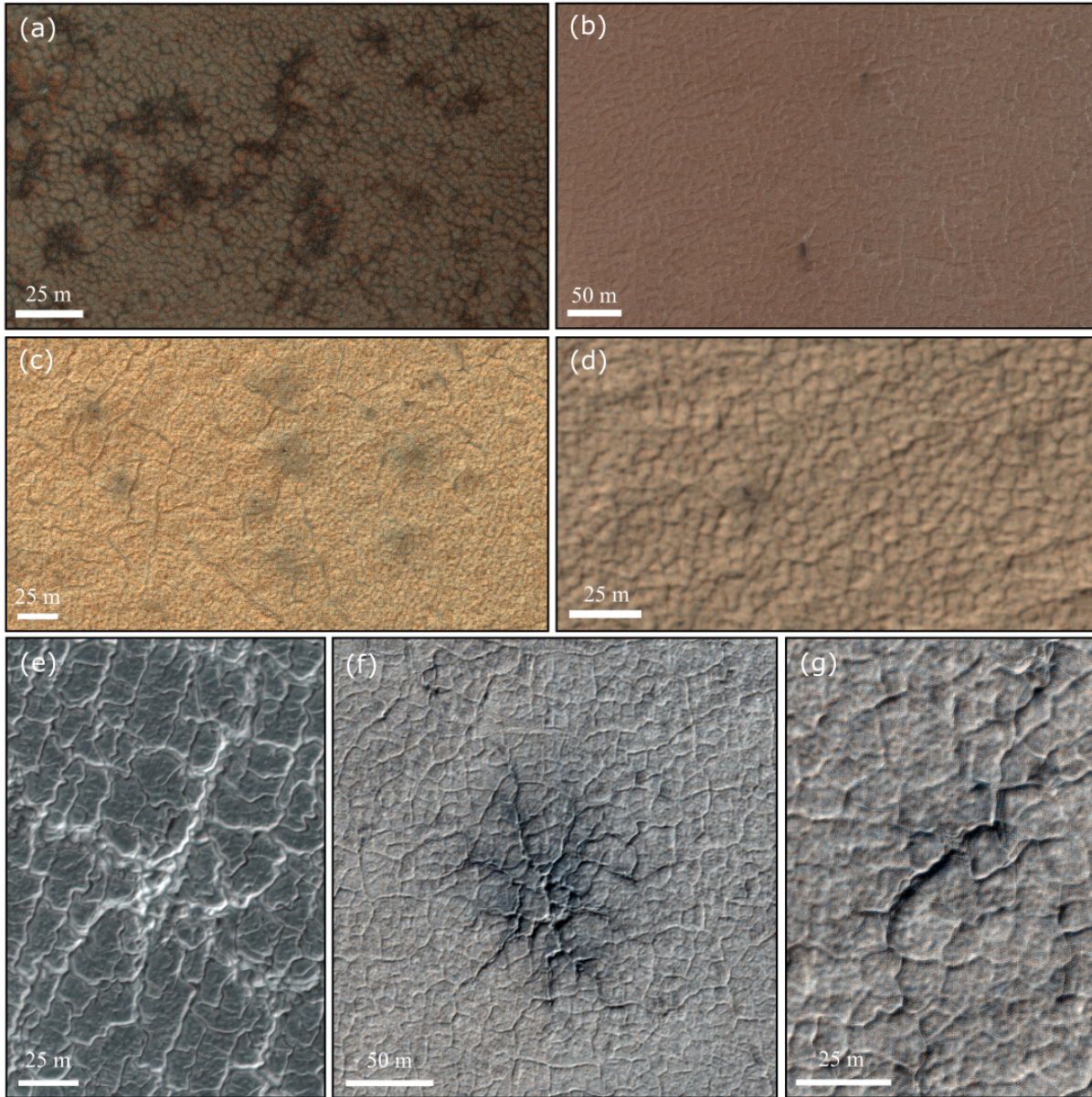


Fig. 2. Martian araneiforms growing on terrains with different polygonal patterns. (a) Araneiforms on a hexagonal-dominated polygon terrain (ESP_052822_2615). (b) Two araneiform structures on a mixed polygon terrain (ESP_011491_0985). (c) A series of araneiforms on a terrain with fine polygonal grids (ESP_066461_0765). (d) Araneiforms on a pentagon-dominated polygon terrain (ESP_066595_0750). (e) The araneiform on a terrain with quadrangular polygons (ESP_056927_0940). (f) The araneiform on a terrain with mixed polygons (ESP_066587_0790). (g) Polygonal relicts with raised rims.

2.2 Morphological analysis

Both the spiders on Mars and in the Qaidam Basin are comparable to the dendritic drainage system and are highly fractal. To quantitatively assess their morphological similarities, we adopt the ordering scheme of streams^[11] in hydrology to determine the order of each araneiform tributary. We count the number of tributaries (N_w) in each order (w) and use them for the linear regression of Horton's law^[21] (a geometric relationship proposed for water diffusion systems):

$$\log_{10} N_w = kw + b, \quad (1)$$

where k and b are the slope and intercept of the regression line, respectively.

We also calculate the R-squared value (R^2) and branching ratio according to the linear fitness results. The R-squared value^[22] varies from 0 to 1, and a larger value indicates a better fit quality of Horton's law. The calculation of the R-squared value is

$$R^2 = 1 - \frac{\sum_w (y_w - kw - b)^2}{\sum_w (y_w - y_{mean})^2}, \quad (2)$$

where $y_w = \log_{10} N_w$, and y_{mean} represents the mean value of y_w .

The branching ratio^[11] is used to distinguish two fractal patterns, i.e., two fractal patterns with the same formation mechanism should have similar branching ratios. To determine the

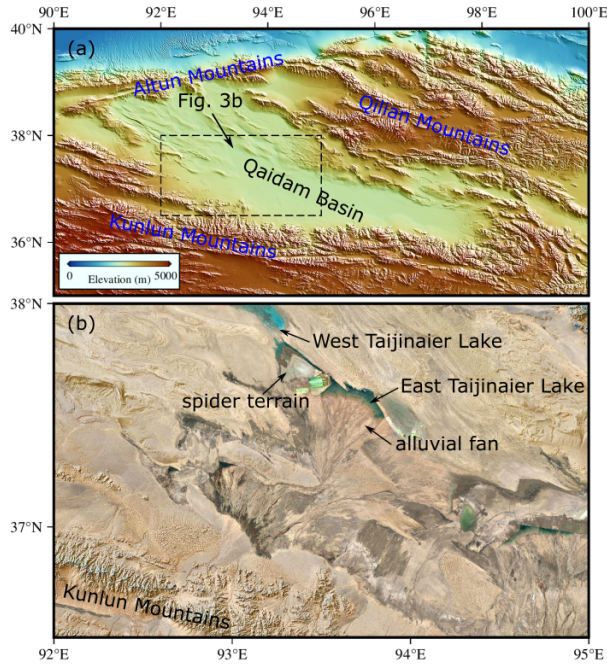


Fig. 3. The geological features of the Qaidam Basin and the observed spider terrain. (a) The shaded relief map of the Qaidam Basin. (b) The geographic background of the spider terrain (Google satellite images taken on November 28th, 2012).

branching ratio (R_b), we have

$$R_b = \log_{10}^{-1} k. \quad (3)$$

2.3 Numerical simulations

The diffusion-limited aggregation (DLA) algorithm^[23] is widely used to simulate natural fractal phenomena with Laplace growth^[24]:

$$\nabla^2 \varphi(\vec{x}) = 0 \quad (4)$$

or Poisson growth modes^[25]:

$$\nabla^2 \varphi(\vec{x}) = f, \quad (5)$$

where \vec{x} , $\varphi(\vec{x})$, and f represent the spatial coordinate, the concentration of aggregated particles, and the imposed constraint, respectively. The DLA method does not directly solve the above partial differential equations but generates fractal aggregation through the random walk of particles. The DLA method is also successfully applied to simulate many water-diffusion fractal networks on Earth^[14, 26]. Because araneiforms exhibit a similar fractal pattern, the DLA method has been previously used to study their growth^[11]. In this study, we build a DLA model to investigate the origin of araneiforms, in particular, the cause of their multiform morphologies under the water-diffusion situation.

Different spider growth situations have been implemented in our numerical model. For the free-growing situation, we use the standard DLA algorithm^[11, 27] to run the simulation. The model is grid-free^[26] and the random walk of some circular tracers is used to approximate the free diffusion of water. The length of the computational domain is nondimensional-

ized by the radius (r_i) of the circular tracer (set to 1). As the DLA method only generates the steady state of a fractal pattern, there is no time scale in our simulations. For the simulations with a point water source, we put a seed tracer in the center of the model domain (Fig. S2a in the Supporting Information). After that, a series of water tracers are released from the model boundary successively and move randomly until they are in contact with the seed tracer or other water tracers. The geometry of the initial water source can also be changed to simulate realistic conditions. A series of seed tracers are set to fill the desired source region before the release of water tracers. For example, we can set an initial line source to approximate a brine ditch and simulate the water diffusion networks branching from it (Fig. S2b in the Supporting Information). For simulation with a pre-existing polygonal network, we need to adapt the standard algorithm. When the water tracer of the araneiform touches the polygonal boundary (called a side tracer) (Fig. S2c in the Supporting Information), we determine the vertex at the polygonal boundary closest to the side tracer. We use additional water tracers to fill the area between the side tracer and the closest vertex so that the araneiform can grow along this polygonal boundary (Fig. S2d in the Supporting Information).

3 Results

3.1 Morphological features of the Qaidam spiders

In the Qaidam Basin, the formation of spiders was due to the upwelling of subsurface salt water from the surface weakness, which diffused around and eroded the surface (Fig. 5a). The continuous supply of salt water and its progressive erosion expand the size of a spider structure from the center outward. Because of the strong evaporation and the limited saltwater supply, the growth of araneiforms may halt, and araneiforms may remain in different stages. As the araneiforms progress from the early stage (Fig. 4a) to the late stage (Fig. 4b), their patterns become more intricate, accompanied by an increase in the number and order of branches. Following the evaporation of salt water, the salts (mainly halite and gypsum) remained in the erosion channels (Figs. 4a–b). We also observed that the channels became narrower and the green-colored salt deposits became lighter from the central source to the edge, indicating a depletion in salt water (Figs. 4a–b).

In addition to the typical starbursts, other spider morphologies can be found in the Qaidam Basin (Figs. 4c–h). Notably, a series of parallel spider channels can be observed (Figs. 4c–d). Unlike a point source, they originate from an artificial saltwater canal (i.e., a linear source) and extend orthogonally. We also observed multiple channels emanating from the edges of a large pit on the site, forming a fat araneiform morphology similar to that on Mars (Fig. 4e). Moreover, some parts of the site retain distinct polygonal ground patterns (Fig. S3 in the Supplementary Materials), where spiders tend to occupy the same channels as the polygonal cracks (Figs. 4f–h).

3.2 Quantitative morphological analysis

We selected 31 Martian araneiforms (Table S1 in the Supplementary Materials) and 5 Qaidam araneiforms (Table S2 in

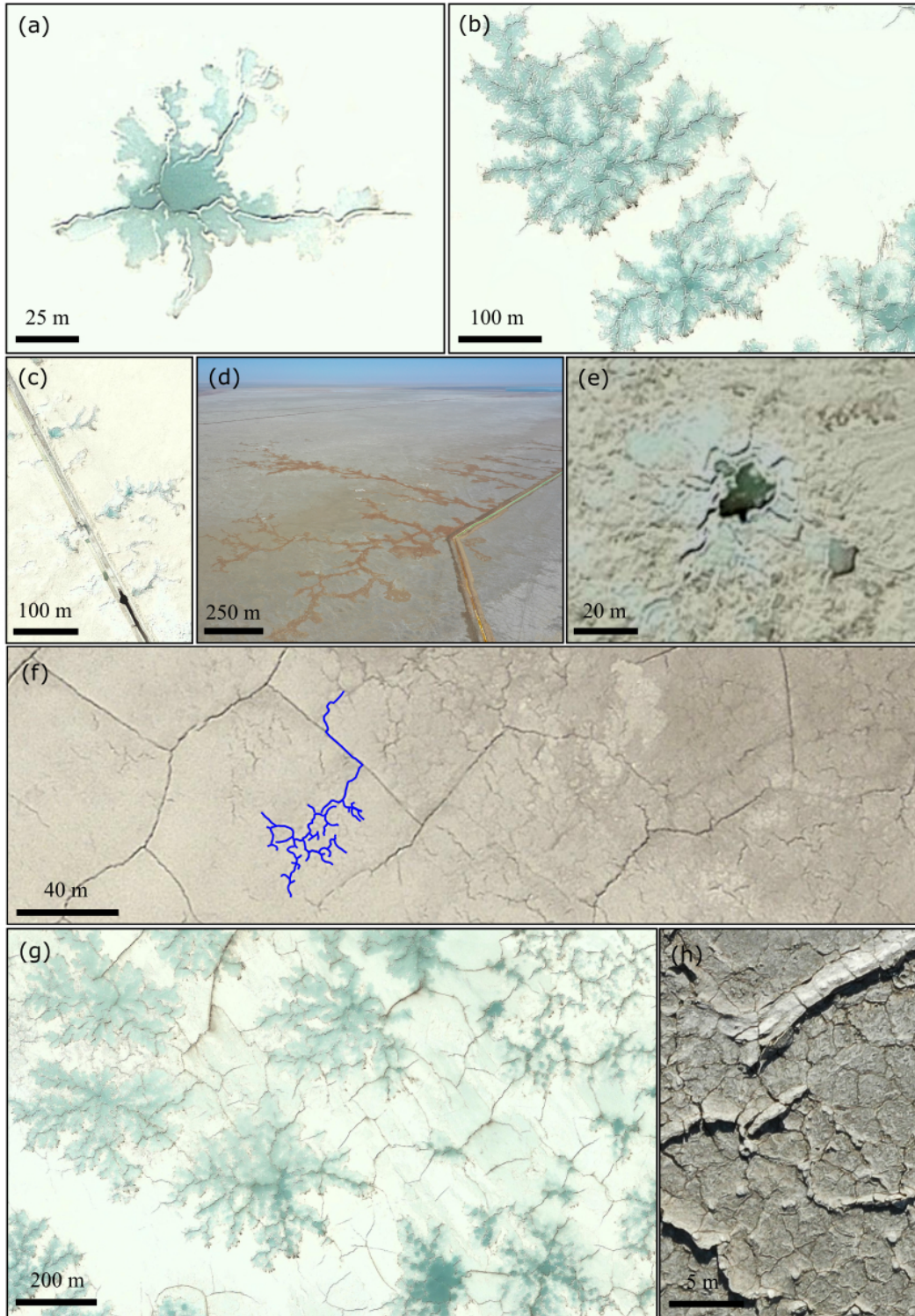


Fig. 4. The Qaidam spiders with different morphologies. (a) The early stage of the Qaidam spider. (b) The middlescence stage of the Qaidam spiders. (c-d) Parallel spiders formed along artificial saltwater canals. (e) A fat spider. Figs. 4a, 4b, 4c & 4e are Google satellite images taken on November 28th, 2012. Fig. 4d is the aerial image taken during our fieldwork in July 2021. (f-g) Spiders growing on a polygonal terrain (Google satellite images taken on November 28th, 2012). (h) Polygonal relics with raised rims (aerial image taken during our fieldwork in July 2021). To clearly show the spider networks, some parts of them in Fig. 4f are marked in blue.

the Supplementary Materials) for fractal analysis (see Materials and methods). Our analysis revealed that all examined structures exhibited a high R-squared value (> 0.98) (Fig. 5b), suggesting that they comply well with Horton's law^[21] and are

analogous to the drainage system. The ranges of their branching ratios also agree well (Fig. 5b), indicating analogous fractal properties. Thus, our results affirm that the aranei-forms in the Qaidam Basin are good morphological analogs to

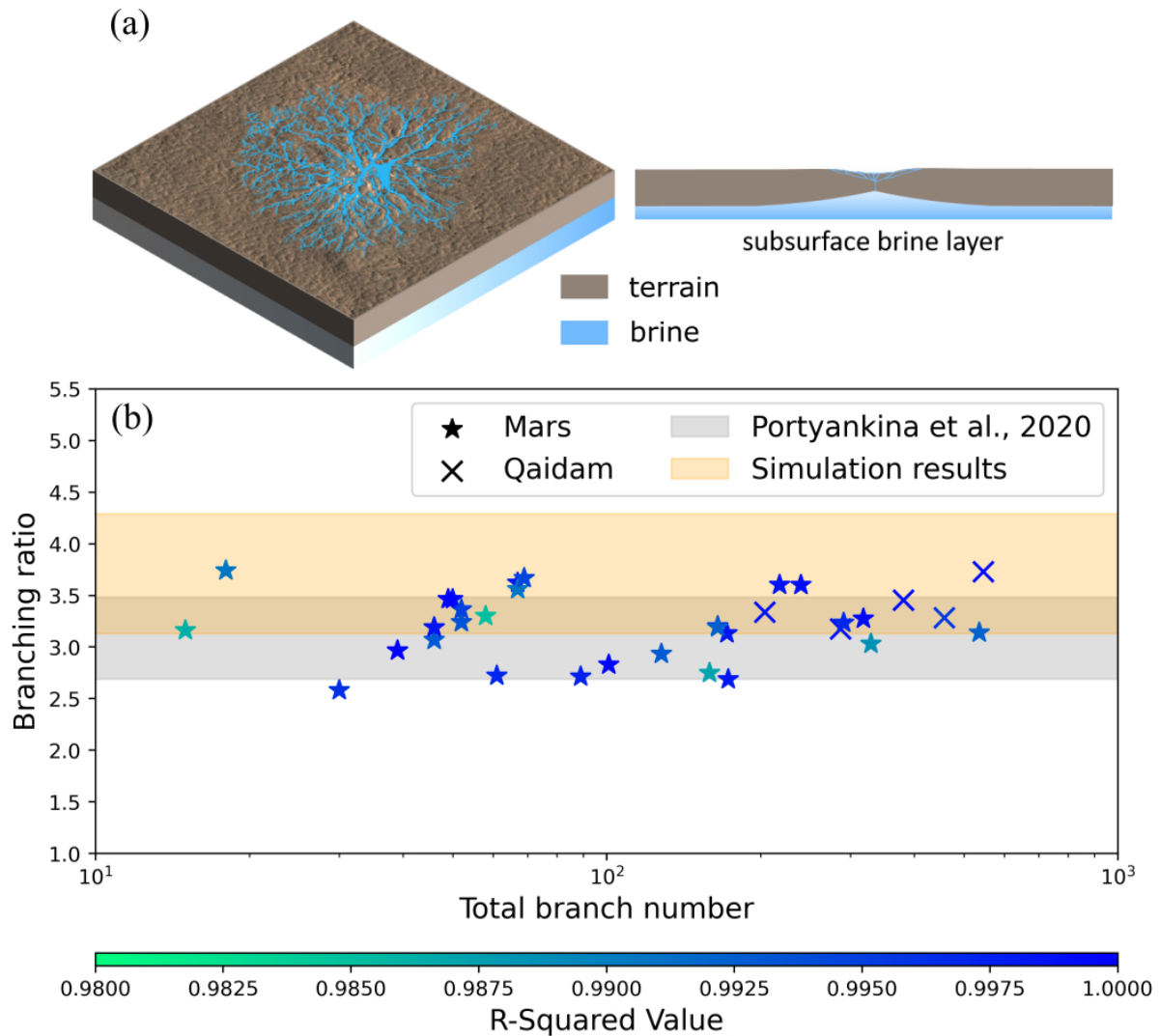


Fig. 5. The formation mechanism and fractal analysis results of araneiforms. (a) The formation mechanism of the Qaidam spiders. The lighting effect is used to enhance the aesthetic appeal of the blue brine. (b) The calculated branching ratios of the selected Martian araneiforms and the Qaidam spiders. The color represents the R-squared value (a larger value means a smaller deviation from Horton's law). The gray area is the range given in a previous study of Martian araneiforms^[10]. The orange region is the range of our DLA simulation results (100 tests for a free-growing araneiform in Fig.6a).

the araneiforms on Mars.

3.3 Simulations of the araneiform growth

The orientation and geometry of water diffusion networks can be significantly influenced by local topographic conditions, which may explain the cause of different spider morphologies. In our simulations, we have examined the effects of various topographic conditions. Under the first condition, we simulate a free-growing araneiform with different source geometries. When a point source is chosen, we obtain a radially symmetric araneiform pattern (Fig. 6a), as seen in conventional Martian araneiforms and Qaidam spiders (Figs. 1a–c & 4a–b). However, when a linear source is chosen, parallel fractal networks develop (Fig. 6b), as observed on Mars and in the Qaidam Basin (Figs. 1e & 4c–d). We also try an elliptical source (e.g., a saltwater pool) and let the araneiform grow from the elliptical edge (Fig. 6c), resulting in features similar to the fat spider on Mars or in the Qaidam Basin (Figs. 1h & 4e). In the second condition, we set a forbidden zone for wa-

ter diffusion (the gray region in Fig. 6d) to simulate a dune with high topography (Fig. 1g) and obtain a semi-spiny spider. In the third condition, we use pre-existing polygonal networks to constrain the growth of the araneiform (Figs. 6e–f). When a channel grows and eventually encounters polygonal cracks, water should preferentially enter and diffuse along the cracks. We consider this orientation bias in the water-diffusion simulation (see Materials and methods) and investigate its possible influence on the araneiform morphology. We use both quadrangular (Fig. 6e) and hexagonal (Fig. 6f) polygonal webs observed on Mars, and the corresponding simulation results differ significantly from the free-growing spider (Fig. 6a). Consistent with observations on Mars and in the Qaidam Basin (Figs. 2 & 4f–g), these araneiforms tend to share their channels with pre-existing polygonal cracks, which may be considered as an important water-diffusion feature.

4 Discussion

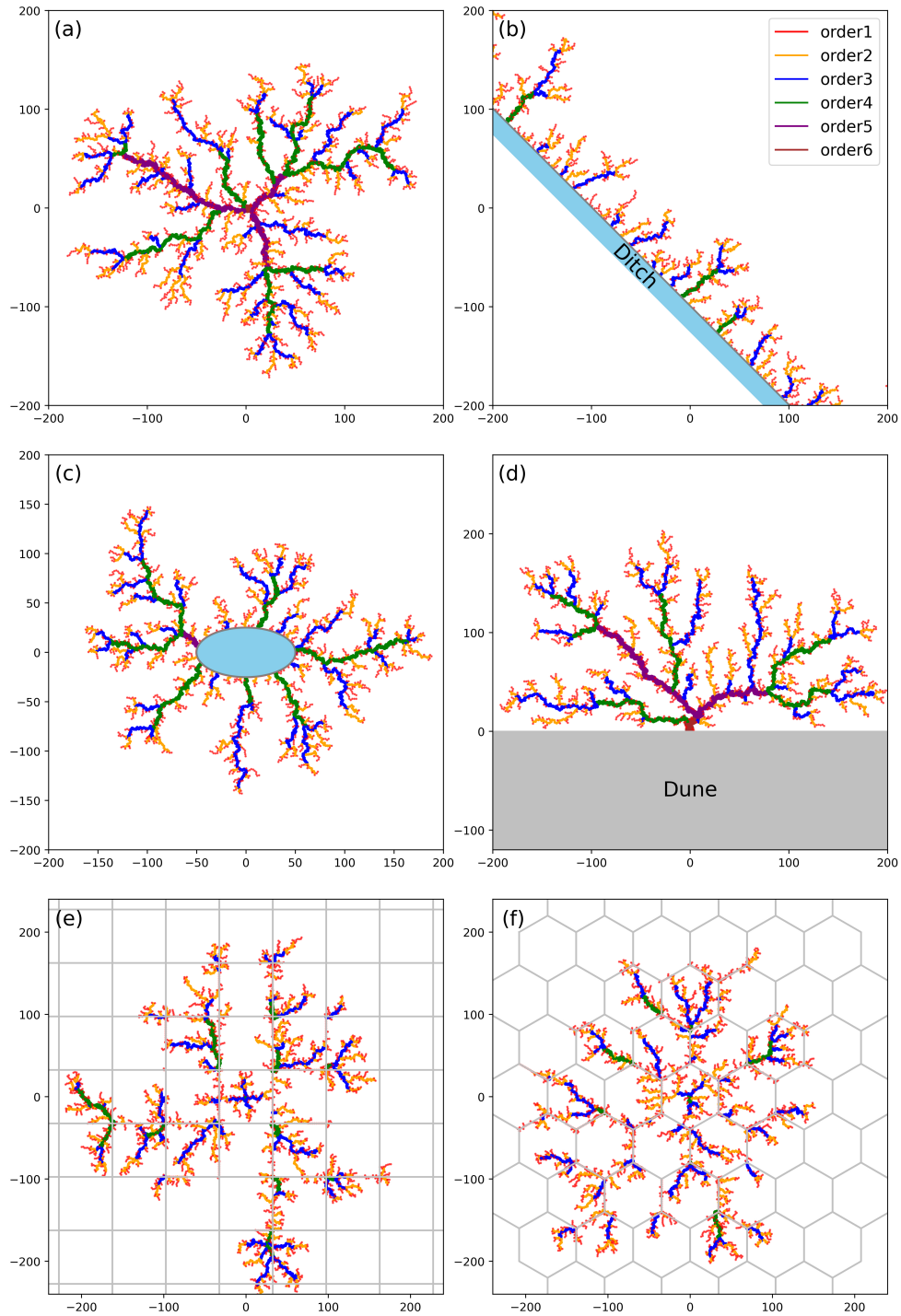


Fig. 6. Simulation results of water-diffusion patterns with different sources and ground conditions. (a) A free-growing araneiform. (b) Parallel araneiforms originating from a ditch. (c) A fat araneiform originating from an upwelling pool. (d) A semi-emergent araneiform in which water diffusion is prohibited in the gray region. (e) The araneiform growing on a pre-existing quadrangular network. (f) The araneiform growing on a pre-existing hexagonal network.

4.1 Qaidam spiders are analogous to Martian araneiforms

Based on the above observations and analysis, we propose that the Qaidam spiders are geomorphological analogs of the Martian araneiforms. They have the same progressive growth forms and comparable sizes at different stages (Figs. 1a–c & 4a–b). From the early stage with only a few branched chan-

nels to the later stage with hundreds of channels, the size of the araneiform varies from a few tens of meters to hundreds of meters. However, larger araneiforms with diameters of several kilometers have not been found in the Qaidam Basin. This could be due to the lack of underground salt water. Before the spider web continues to grow, the supply of upwelling salt water dries up. Furthermore, the morphological

characteristics of Qaidam spiders match those of Martian araneiforms under different topological conditions. On both the Martian and Qaidam, there are parallel araneiforms (Figs. 1e & 4c–d), fat araneiforms (Figs. 1h & 4e), and twisted araneiforms (Figs. 2 & 4f–h) that arise from pre-existing burrows, pits, and polygonal webs, respectively.

From a fractal geometric perspective, both the Qaidam spiders and the Martian araneiforms conform to Horton's law (Fig. 5b), indicating their nature as water-diffusion systems. Fractal analysis reveals that they have similar branching ratios (Fig. 5b), providing quantitative confirmation of their analogy. We note that there is a small systematic deviation in the branching ratio between the simulation results (the orange region in Fig. 5b) and the observation. This divergence could be due to the bias in the conservation of the araneiform channels. Compared with the high-order channels, the low-order channels are generally narrower and shallower, so they are more easily obliterated by wind erosion. As the maturity and branching number increase, the influence of this distortion weakens. Therefore, the araneiform with more branches is closer to the simulation results and has a higher branching ratio (Fig. 5b).

4.2 A saltwater-related model for araneiform formation

The analogy between the Qaidam spiders and the Martian araneiforms suggests that they may have a similar saltwater-related origin. As observed with the Qaidam spiders, the formation of the araneiforms on Mars may also have been caused by the upwelling subsurface salt water that flows out, spreads, dissects the terrain, and creates fractal networks (Fig. 5a). The incessant upwelling of subsurface salt water separated the outflows from the previous network and the araneiform was enlarged accordingly.

Based on the observational and simulation results, water-diffusion processes and the resulting araneiform morphology are significantly influenced by ground conditions, such as local topography and pre-existing structures. This scenario is consistent with the formation of half spiders below the floor of a dune (Figs. 1g & 6d), which is driven by gravity and cannot grow upward from the bottom of the dune. Consequently, it can only grow on one side and form a semi-growth pattern. Araneiforms growing at the base of a pre-existing ditch often form a series of parallel dendritic webs (Figs. 1e, 4c–d & 6b). They typically grow in a direction perpendicular to the ditch, like tributaries separated from the mainstream. Moreover, if a pit already exists, the upwelling salt water may flow out of the pit and diffuse from its rim to form fat spiders (Figs. 1h, 4e & 6c). An alternative mechanism for fat spider formation may be erosion by surface salt water^[28]. Some salt water may remain on the surface after it has risen from the subsurface. The surface salt water tends to flow into a depression like a pit. The accumulation of the water flows could create converging troughs around the pit and make a fat spider. On the polygonal terrain, the water preferentially diffuses along the polygonal fractures and the araneiform network overlaps the pre-existing polygonal network (Figs. 2, 4f–h & 6e–f). This orientation mismatch could also explain why the araneiforms growing on the polygonal terrain with different geometries have different morphologies (Figs. 2, 4f–h & 6e–f).

4.3 Implications for the water search on Mars

The search for water is one of the most important scientific missions in the exploration of Mars^[29–36]. According to recent satellite observations, the growth of araneiforms is still active in some areas of the southern hemisphere of Mars^[3]. If the araneiforms originate from subsurface salt water, this salt water should still be active in the subsurface environments of these regions. Some laboratory experiments have shown that the salt solutions of ion mixtures can have a melting point lower than 220 K^[28]. In addition, a temperature model of the Inca City (a Martian spider terrain with a latitude of ~ 81°S) suggests that the highest summer temperature can reach ~258 K, which is possible for the existence of liquid salt water^[28].

5 Conclusions

In summary, this study proposes that the spider structures observed in the Qaidam Basin are geomorphological analogs of the Martian araneiforms. The formation of Qaidam spiders is caused by the erosion of upwelling saltwater from the subsurface. This saltwater-related mechanism can also be used to explain the formation of Martian araneiforms with diverse morphological features. These findings provide new insights into the origin of araneiforms and have significant implications for future water searches on Mars.

Supporting information

The supporting information for this article can be found online at <http://doi.org/10.52396/JUST-2023-0164>. It includes three figures (Figs. S1–S3) and two tables (Tables S1–S2).

Acknowledgements

This work was supported by the Strategic Priority Research Program of the Chinese Academy of Sciences (XDB41000000) and the Fundamental Research Funds for the Central Universities (WK2080000144). We thank the USTC Supercomputing Center for providing computational resources for this project. We thank Dr. B.L. Ye, Dr. Y. Sun, Mr. J.M. Zhu, Dr. T.L. Zhao, Mr. Z.K. Li, Dr. Y.H. Qi, and Dr. W.P. Liu for their invaluable assistance in the field. The code and data used in this study are available in Zenodo (<https://doi.org/10.5281/zenodo.7919430>). The images of the Martian araneiforms are available at www.uahirise.org, and the image ID is given in the figure captions. The satellite pictures of the Qaidam Basin can be obtained from Google Earth (<https://earth.google.com>).

Conflict of interest

The authors declare that they have no conflict of interest.

Biographies

Shengxing Zhang is a Ph.D. candidate at the University of Science and Technology of China. His research mainly focuses on numerical simulations, geodynamics, and Martian analogs.

Yiliang Li is an Associate Professor at the University of Hong Kong. He received his Ph.D. degree from the University of Science and

Technology of China in 1999. His two research interests are in the general field of astrobiology, including the mineral records of the early life on Earth and Martian analogs.

Wei Leng is a Professor at the University of Science and Technology of China. He received his Ph.D. degree from the University of Colorado Boulder in 2010. His research mainly focuses on geodynamics and planetary science.

References

- [1] Hao J, Michael G G, Adeli S, et al. Araneiform terrain formation in Angustus Labyrinthus, Mars. *Icarus*, **2019**, *317*: 479–490.
- [2] Hansen C J, Thomas N, Portyankina G, et al. HiRISE observations of gas sublimation-driven activity in Mars' southern polar regions: I. Erosion of the surface. *Icarus*, **2010**, *205* (1): 283–295.
- [3] Portyankina G, Hansen C J, Aye K-M. Present-day erosion of Martian polar terrain by the seasonal CO₂ jets. *Icarus*, **2017**, *282*: 93–103.
- [4] Piqueux S, Byrne S, Richardson M I. Sublimation of Mars's southern seasonal CO₂ ice cap and the formation of spiders. *Journal of Geophysical Research: Planets*, **2003**, *108* (E8): 5084.
- [5] Kieffer H H, Christensen P R, Titus T N. CO₂ jets formed by sublimation beneath translucent slab ice in Mars' seasonal south polar ice cap. *Nature*, **2006**, *442* (7104): 793–796.
- [6] Kieffer H H, Titus T N, Mullins K F, et al. Mars south polar spring and summer behavior observed by TES: Seasonal cap evolution controlled by frost grain size. *Journal of Geophysical Research: Planets*, **2000**, *105* (E4): 9653–9699.
- [7] Hao J, Michael G G, Adeli S, et al. Variability of spider spatial configuration at the Martian south pole. *Planetary and Space Science*, **2020**, *185*: 104848.
- [8] Piqueux S, Christensen P R. North and south subice gas flow and venting of the seasonal caps of Mars: A major geomorphological agent. *Journal of Geophysical Research: Planets*, **2008**, *113* (E6): E06005.
- [9] Schwamb M E, Aye K-M, Portyankina G, et al. Planet Four: Terrains—Discovery of araneiforms outside of the South Polar layered deposits. *Icarus*, **2018**, *308*: 148–187.
- [10] Mc Keown L E, Diniega S, Bourke M C, et al. Morphometric trends and implications for the formation of araneiform clusters. *Earth and Planetary Science Letters*, **2023**, *607*: 118049.
- [11] Portyankina G, Hansen C J, Aye K-M. How Martian araneiforms get their shapes: morphological analysis and diffusion-limited aggregation model for polar surface erosion. *Icarus*, **2020**, *342*: 113217.
- [12] De Villiers S, Nermoen A, Jamtveit B, et al. Formation of Martian araneiforms by gas-driven erosion of granular material. *Geophysical Research Letters*, **2012**, *39* (13): L13204.
- [13] Mc Keown L, McElwaine J N, Bourke M C, et al. The formation of araneiforms by carbon dioxide venting and vigorous sublimation dynamics under Martian atmospheric pressure. *Scientific Reports*, **2021**, *11* (1): 6445.
- [14] Masek J G, Turcotte D L. A diffusion-limited aggregation model for the evolution of drainage networks. *Earth and Planetary Science Letters*, **1993**, *119* (3): 379–386.
- [15] Dang Y, Xiao L, Xu Y. Polygons. In: Mars on Earth: A study of the Qaidam Basin. Singapore: World Scientific, **2021**: 199–247.
- [16] Lai Z, Mischke S, Madsen D. Paleoenvironmental implications of new OSL dates on the formation of the “Shell Bar” in the Qaidam Basin, northeastern Qinghai-Tibetan Plateau. *Journal of Paleolimnology*, **2014**, *51* (2): 197–210.
- [17] Anglés A, Li Y. The western Qaidam Basin as a potential Martian environmental analogue: An overview. *Journal of Geophysical Research: Planets*, **2017**, *122* (5): 856–888.
- [18] Li J, Li T, Ma Y, et al. Distribution and origin of brine-type Li-Rb mineralization in the Qaidam Basin, NW China. *Science China Earth Sciences*, **2022**, *65* (3): 477–489.
- [19] Xiao L et al. A new terrestrial analogue site for Mars research: The Qaidam Basin, Tibetan Plateau (NW China). *Earth-Science Reviews*, **2017**, *164*: 84–101.
- [20] Zhao J, Shi Y, Xiao L. Valleys. In: Mars on Earth: A study of the Qaidam Basin. Singapore: World Scientific, **2021**: 249–273.
- [21] Horton R E. Erosional development of streams and their drainage basins; hydrophysical approach to quantitative morphology. *Geological Society of America Bulletin*, **1945**, *56* (3): 275–370.
- [22] Chicco D, Warrens M J, Jurman G. The coefficient of determination R-squared is more informative than SMAPE, MAE, MAPE, MSE and RMSE in regression analysis evaluation. *PeerJ Computer Science*, **2021**, *7*: e623.
- [23] Witten T A, Sander L M. Diffusion-limited aggregation, a kinetic critical phenomenon. *Physical Review Letters*, **1981**, *47* (19): 1400–1403.
- [24] Sui S G, Gong S L, Wang T. Study on Laplace growth and diffusion limited aggregation with material properties. *Advanced Materials Research*, **2013**, *703* (2): 71–74.
- [25] La Roche H, Fernández J F, Octavio M, et al. Diffusion-limited-aggregation model for Poisson growth. *Physical Review A*, **1991**, *44* (10): R6185–R6188.
- [26] Wang S, Ji H, Zhang Y, et al. Research on the model improvement of a DLA fractal river network. *IEEE Access*, **2020**, *8*: 100702–100711.
- [27] Halsey T C. Diffusion-limited aggregation: A model for pattern formation. *Physics Today*, **2000**, *53* (11): 36–41.
- [28] Prieto-Ballesteros O, Fernández-Remolar D C, Rodríguez-Manfredi J A, et al. Spiders: Water-driven erosive structures in the southern hemisphere of Mars. *Astrobiology*, **2006**, *6* (4): 651–667.
- [29] Boynton W V, Feldman W C, Squyres S W, et al. Distribution of hydrogen in the near surface of Mars: Evidence for subsurface ice deposits. *Science*, **2002**, *297* (5578): 81–85.
- [30] Bridges J C, Schwenzer S P. The nakhlite hydrothermal brine on Mars. *Earth and Planetary Science Letters*, **2012**, *359–360*: 117–123.
- [31] Rivera-Valentín E G, Gough R V, Chevrier V F, et al. Constraining the potential liquid water environment at Gale Crater, Mars. *Journal of Geophysical Research: Planets*, **2018**, *123* (5): 1156–1167.
- [32] Cassanelli J P, Head J W. Lava heating and loading of ice sheets on early Mars: Predictions for meltwater generation, groundwater recharge, and resulting landforms. *Icarus*, **2016**, *271*: 237–264.
- [33] Li C, Zheng Y, Wang X, et al. Layered subsurface in Utopia Basin of Mars revealed by Zhurong rover radar. *Nature*, **2022**, *610* (7931): 308–312.
- [34] Ojha L, Wilhelm M, Murchie S, et al. Spectral evidence for hydrated salts in recurring slope lineae on Mars. *Nature Geoscience*, **2015**, *8* (11): 829–832.
- [35] Dundas C M, Bramson A M, Ojhal L, et al. Exposed subsurface ice sheets in the Martian mid-latitudes. *Science*, **2018**, *359* (6372): 199–201.
- [36] Carr M H. The fluvial history of Mars. *Philosophical Transactions of the Royal Society A: Mathematical, Physical and Engineering Sciences*, **2012**, *370* (1966): 2193–2215.